HYDROGEN EVOLUTION MEASUREMENTS FOR A MARTENSITIC-AUSTENITIC WELD METAL

T. Kasuya, Y. Hashiba and H. Inoue

ABSTRACT

Hydrogen evolutions for martensitic-austenitic weld metals were measured at 45 °C. The specimen without the austenite released hydrogen in about two days, and this result agrees with the 72 h holding time required by JIS Z3118. In the case of the specimens that contain the retained austenite, hydrogen release continued for about 100 days or more. We derived the analytic solution of the McNabb & Foster diffusion equation by regarding the austenitic microstructures as trapping sites to compare the experimental and calculation results, and showed that both of them are in good agreement. We also showed that the initial ratio of free and trapped hydrogen atoms is not necessarily equal to the thermal equilibrium condition at the measurement temperature, which can be analysed using the present solution.

IIW-Thesaurus keywords: Austenite; Hydrogen; Martensite.

1 Introduction

Preheating is a very effective method to avoid cold cracking in the HAZ when steels with high cold cracking susceptibility are welded. The purpose of preheating is to accelerate hydrogen diffusion and to release hydrogen from the welded joint. As the strength of steels becomes high, the hydrogen content after the completion of welding must be reduced, and hence the necessary preheat temperature tends to become high.

On the other hand, high preheating means low efficiency of welding works, and hence, the reduction of preheat temperature, especially for high-strength steels, is strongly desired. The authors are carrying on the activities of the project "Fundamental Studies on Technologies for Steel Materials with Enhanced Strength and Functions", and developing welding wires of 980 MPa grade that can be used without preheating. The basic idea is that the retained austenite and the martensite are introduced to trap diffusible hydrogen and to increase the strength, respectively. In general, austenitic microstructure is well-known beneficial to prevent cold cracking [1], but no welding consumables with a strength as high as 980 MPa that can be used without preheating have ever existed.

When there is the trap effect in the weld metal, the hydrogen evolution phenomena (outgassing from the welded joint) are influenced. But few experimental results about the hydrogen evolution from the austenitic weld metals exist [2], and no results have been obtained for the 980 MPa grade weld metal. In this work, we examine the hydrogen evolution curves from the weld metals. The hydrogen is charged with a TIG torch using Ar + 5 % H_2 as the shielding gas. The diffusion analysis using the McNabb & Foster Equation [3] is also shown.

2 Experimental procedures

We first prepared the three plates whose chemical compositions are shown in Table 1. The laboratory melted ingots were rolled to a 10 mm thickness and kept at 1 200 °C for 24 h and then cooled in the furnace. To introduce the weld metals into the plates, we conducted TIG welding. The welding conditions are shown in Table 2, and we did not use any welding wires. In order to charge hydrogen, the Ar + 5 % H_2 gas mixture was used as the shielding gas. Since no welding wire was used, the chemical compositions of the weld metals produced by the TIG welding are the same as those shown in Table 1. In Table 1, Specimens A and B contain some amount of austenitic microstructures as shown later. Both of them contain considerably high amounts of Cr and Ni. On the other hand, Specimen C is considered to contain no austenite. Specimen C has been selected to compare to Specimens A and B. The test piece size was 10 mm × 25 mm × 40 mm. We also prepared conventional 490 MPa grade steel plates of 10 mm × 25 mm × 30 mm. These were used as tab plates. TIG welding was conducted to introduce hydrogen.

According to the Japanese industrial standard, JIS Z3118, the specimen was kept in liquid nitrogen after completion of welding, and heated to room temperature and immediately inserted in the hydrogen collection cell and kept at 45 °C. This procedure means that the specimen was

Doc. IIW-2183, recommended for publication by Commission IX "Behaviour of Metals Subjected to Welding."

Table 1 – Chemical compositions of the specimens [wt. %]

Specimen	C	Si	Mn	Cr	Ni	Mo	Retained austenite percentage [a]	Initial hydrogen content [b] [ml/100 g W.M.]
A	0.045	0.33	0.83	14.1	9.3	-	16	6.7
B	0.026	0.34	0.82	14.0	8.2	-	8	7.1
C	0.075	0.50	1.80	1.1	2.9	0.64	-	6.5

[a] *The retained austenite percentage was measured by the X-ray method after TIG welding and quenching in liquid nitrogen.*
[b] *The initial hydrogen content introduced by TIG welding with Ar + 5 % H_2 shielding gas.*

Table 2 – TIG welding conditions

Current [A]	Voltage [V]	Speed [cm/min]	Shielding gas
180	13	10	Ar + 5 % H_2

cooled down to −196 °C. This procedure might influence the microstructure of the specimen. Hence, the specimen was examined by X-ray method to detect the volumetric ratio of the austenitic microstructures. The hydrogen evolution curves were measured by measuring the amount of hydrogen outgassing from the specimen. During the first seven days, the measurement was conducted every 24 h, but after that, the measurement interval was set to be 168 h or more. During the measurements, the hydrogen collection cells were kept at 45 °C. The three test pieces of each specimen for the hydrogen measurement were used for the same conditions, and the experimental results were determined as the average values.

3 Experimental results

Figure 1 shows the cross-macrosection of Specimen C. The weld metal was located at the centre of the surface and as shown in Figure 1 the dimensions of the weld metal were approximately 1.6 mm x 9.5 mm. The weld metal size of Specimens A and B was almost the same. These dimensions will be used later. At first, hydrogen was introduced into the weld metal by TIG welding, and released from the specimen or diffused out of the weld metal. Figure 2 shows the experimental hydrogen evolution curves for Specimens A, B and C. In Figure 2, to make comparisons easier, hydrogen on the Y axis was normalized with the total amount of evolved hydrogen. The total amount of evolved hydrogen for each specimen is shown as the initial hydrogen content in Table 1, defined as the hydrogen gas volume in the 100 g weld metal at 0 °C and one atmospheric pressure. From Table 1, we can recognize that the amounts of hydrogen introduced by TIG welding are almost the same for the three specimens even though the chemical compositions are considerably different.

Figure 2 shows that Specimen C released all the hydrogen within 48 h. According to JIS Z3118, it is required to keep specimens at 45 °C for 72 h, and the result shown in Figure 2 agrees with this requirement fairly well. On the other hand, a much longer time period than 72 h is necessary for Specimens A and B to release all the hydrogen. And though the chemical compositions of Specimens A and B are not so different, the time period to release all the hydrogen is quite different (about 5 months for Specimen A and about 3.5 months for Specimen B). Figure 3 shows the microstructures of Specimens A, B and C. The microstructures of Specimens A and B are similar, while that of Specimen C is different. We consider that the slow hydrogen release of Specimens A and B is due to the retained austenite, but it is difficult to show the volume fractions of Specimens A and B from Figure 3. Table 1 also shows the volume fractions measured by the X-ray method after liquid nitrogen quenching. We can see that the retained austenite percentage of Specimen A is twice as high as that of Specimen B. Hence, it is considered that the retardation of hydrogen diffusion is due to the retained austenite and that the difference in hydrogen releases in Specimens A and B is caused by the difference in the volume fraction.

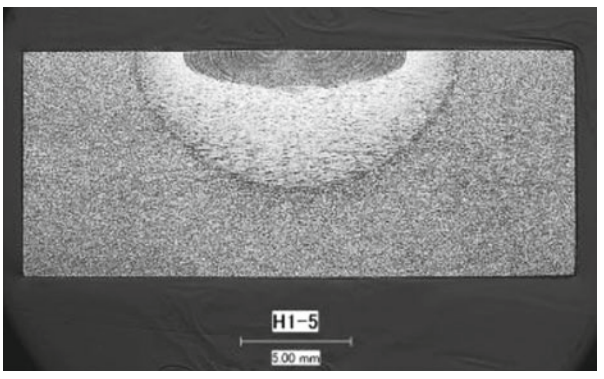

Figure 1 – Cross-section of Specimen C

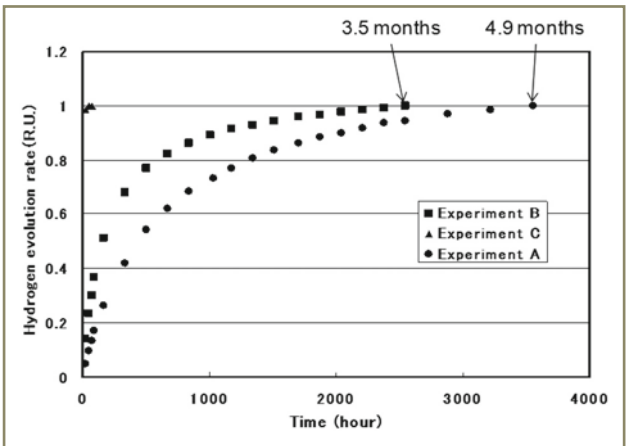

Figure 2 – Experimental results of hydrogen evolution curves

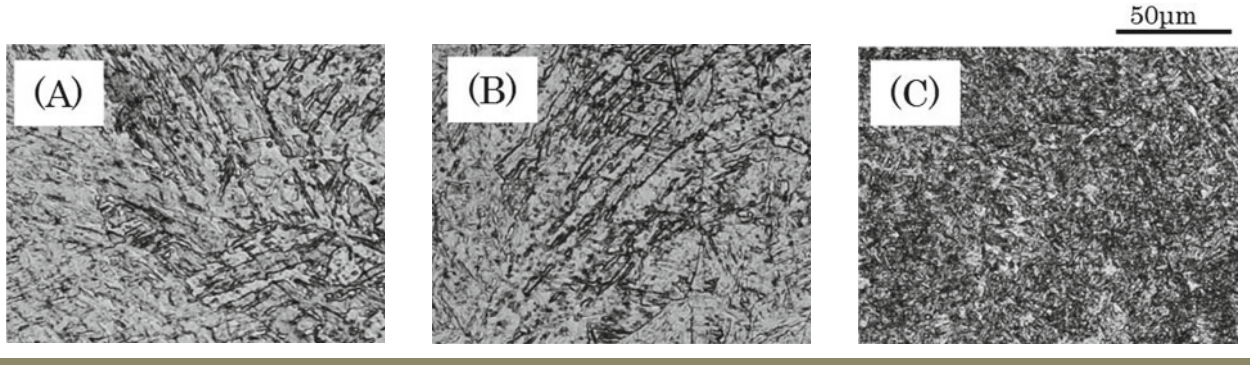

Figure 3 – Microstructures of Specimens A, B and C

4 Discussions

4.1 Selection of diffusion equations

Hydrogen diffusion is generally analysed using Fick's Equation [4], which is described like Equation (1), and since Equation (1) has the same mathematical form of heat conduction equation, Equation (1) has the advantage that we can utilize the results of the heat conduction analysis [5].

$$\frac{\partial c}{\partial t} = D_a \nabla'^2 c \tag{1}$$

where

c is the hydrogen concentration,

t is time [s];

D_a is the apparent diffusion coefficient [mm^2/s],

$$\nabla'^2 = \frac{\partial^2}{\partial x'^2} + \frac{\partial^2}{\partial y'^2} + \frac{\partial^2}{\partial z'^2},$$

x', y', z' are the Cartesian coordinates [mm].

However, Fick's Equation does not discriminate between trapped and free hydrogen atoms. In welding, heat conduction and hydrogen diffusion occur at the same time. In general, the diffusion coefficient of heat conduction is much higher than that of hydrogen diffusion. In this work, the specimens were quenched in ice water just after completion of welding, immediately followed by the liquid nitrogen quenching. Then the hydrogen measurement was conducted keeping the specimens at 45 °C. In this procedure, the cooling rate is quite high, and hence it is considered that the equilibrium state of the considerably high temperature is still held at the beginning of the hydrogen measurement. This means that the initial hydrogen distribution is not necessarily equal to the thermal equilibrium state at the measurement temperature (45 °C in this study) in the case of welded joints.

Like Fick's Equation, McNabb & Foster Equation [3] is also frequently used for diffusion analysis. This equation includes the trap term and the equation consists of the following two parts.

$$\frac{\partial c}{\partial t} + N\frac{\partial \theta}{\partial t} = D\nabla'^2 c \tag{2}$$

$$\frac{\partial \theta}{\partial t} = kc - p\theta \tag{3}$$

where

c is the concentration of free hydrogen atoms,

D is the diffusion coefficient for the case that no trap sites exist,

N is the trap site density per unit volume,

k is the rate constant of capture in the trap sites,

p is the rate constant of escape from the trap sites,

θ is the coverage ratio of the trap sites.

Figure 4 shows the physical concepts p and k which are the rates from the trap site and from the normal site, respectively. In this work, the trap site means the retained austenite and the normal site means the martensite. Here, when the qualities of the martensitic structure in Specimens A and B can be assumed to be equal to each other, the values of p and k for Specimens A and B are the same. The values of N for Specimens A and B are different. It should be emphasized that the value of c, hydrogen concentration, is not that of total hydrogen atoms but that of free hydrogen atoms. The concentration of the trapped hydrogen atoms is $N\theta$. The McNabb & Foster Equation

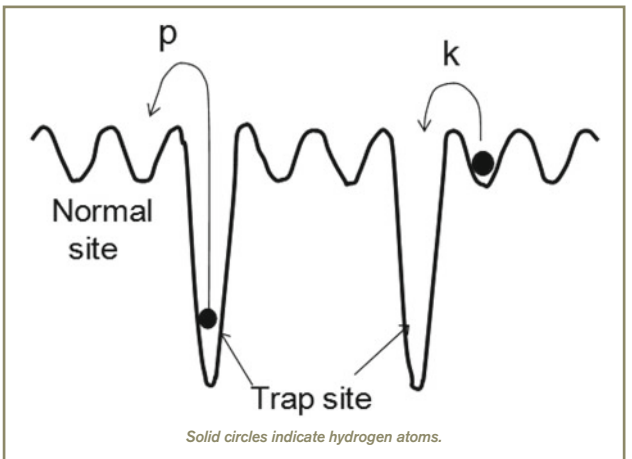

Figure 4 – Illustration of trap and normal sites

has the mathematical form of simultaneous equations, and it is more complicated to derive its analytic solution than to derive the solution of Fick's Equation. However, since the McNabb & Foster Equation can distinguish the free hydrogen atoms from the trapped atoms, it can also discriminate between initial trapped and free atoms.

Here, we would like to compare Fick's Equation with Equations (2) and (3). The left side of Equation (3) means the time change of the coverage ratio of trap sites, which is very low at the local equilibrium condition. Hence, we obtain,

$$\theta = \frac{k}{p}c, \text{ i.e., } \frac{\partial\theta}{\partial t} = \frac{k}{p}\frac{\partial c}{\partial t} \tag{4}$$

Substituting Equation (4) into Equation (2) yields the following equation.

$$\frac{\partial c}{\partial t} = \frac{D}{1+Nk/p}\nabla'^2 c \tag{5}$$

Here, we assume the following relation.

$$D_a = \frac{D}{1+Nk/p}$$

Then, Equation (5) becomes identical to Equation (1). In Equation (5), the value of c means the concentration of free hydrogen atoms, but the same equation is valid for the concentration of total hydrogen atoms as long as the local equilibrium assumption is valid. From the McNabb & Foster Equation, the concentration of total hydrogen atoms, c_T, is described as $c + N\theta = c(1 + Nk / p)$ (since $\theta = kc / p$), which means that c_T is always proportional to c. Hence, by multiplying c in Equation (5) by $(1 + Nk / p)$, Equation (5) can be easily converted to the diffusion equation for the total hydrogen atoms.

From this consideration, it is clear that Fick's Equation assumes the constant ratio of free and trapped hydrogen atoms throughout the diffusion process. The initial ratio of trapped and free atoms is hence determined by this value. As mentioned already, it is not clear that the initial hydrogen distribution is determined by the thermal equilibrium state at the measurement temperature because of the rapid cooling of the specimen. In other words, the hydrogen distribution cannot follow the cooling process. In this work, we would like to examine the effect of the initial ratio of trapped and free atoms, and hence, we selected the McNabb & Foster Equation to analyse the present experimental results.

4.2 Derivation of the analytic solution

Here, we would like to derive the analytic solution of the McNabb & Foster Equation. Firstly, Equations (2) and (3) are normalized

$$\frac{\partial u}{\partial \tau} + \frac{\partial v}{\partial \tau} = \nabla^2 u \tag{6}$$

$$\frac{\partial v}{\partial \tau} = \alpha u - \beta v \tag{7}$$

where

$$u = \frac{c}{c_0},\ v = \frac{N\theta}{c_0},\ \tau = \frac{Dt}{a^2},\ \alpha = \frac{Nka^2}{D},\ \beta = \frac{pa^2}{D},$$
$$\nabla^2 = \frac{\partial^2}{\partial x^2} + \frac{\partial^2}{\partial y^2} + \frac{\partial^2}{\partial z^2},\ x = \frac{x'}{a},\ y = \frac{y'}{a},\ z = \frac{z'}{a}. \tag{8}$$

c_0 is the initial free hydrogen content in the weld metal,

a is the thickness of the specimen.

The parameters b', h', w' and d', that determine the size of the specimen are shown in Figure 5. To normalize the diffusion equation, we also introduce the following parameters.

$$b = b' / a,\ h = h' / a,\ w = w' / a,\ d = d' / a.$$

The hydrogen diffusion model in the present work is shown in Figure 5, where the hatched area corresponds to the weld metal produced by TIG welding and we assume that hydrogen atoms initially existed in this area only. At $t = 0$, the atoms do not exist in the other areas in Figure 5. Then, the initial condition is described as follows.

$$u = 1,\ v = v_0 \text{ (inside the hatched area)}$$
$$u = v = 0 \text{ (outside the hatched area)} \tag{9}$$

We assume that the hydrogen atoms which reach the surface immediately escape from the specimen. Hence, the boundary condition is as follows.

$$u = v = 0 \text{ (at the surface)} \tag{10}$$

Equations (6) and (7) should be solved under the conditions of Equations (9) and (10), and in the present work, we selected the variable separation method.

$$v = \frac{\alpha}{\beta - \mu}\exp(-\mu\tau)X(x)Y(y)Z(z) \tag{11}$$

In Equation (11), it is assumed that v can be described as the multiple form of each independent variable function. Here, μ is a constant, but its value has not been determined yet. The coefficient in the right side, $\alpha / (\beta - \mu)$, has been introduced for the mathematical convenience. Substituting Equation (11) into Equation (7) yields,

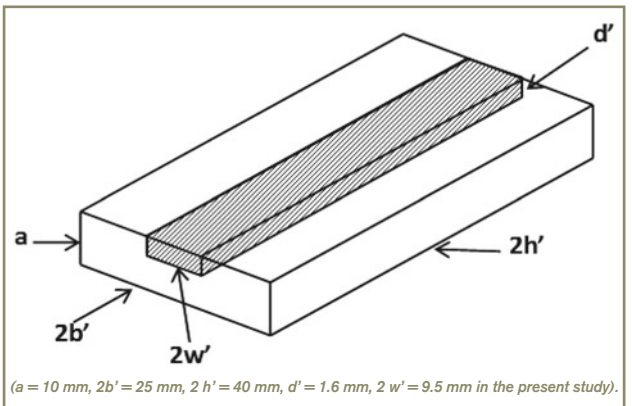

(a = 10 mm, 2b' = 25 mm, 2 h' = 40 mm, d' = 1.6 mm, 2 w' = 9.5 mm in the present study).

Figure 5 – Diffusion model of the present work

$$u = \exp(-\mu\tau)X(x)Y(y)Z(z) \tag{12}$$

We also substitute Equations (11) and (12) into Equation (6) and obtain,

$$-\mu\frac{\alpha+\beta-\mu}{\beta-\mu} = \frac{1}{X(x)}\frac{d^2X(x)}{dx^2} + \frac{1}{Y(y)}\frac{d^2Y(y)}{dy^2} + \frac{1}{Z(z)}\frac{d^2Z(z)}{dz^2} \tag{13}$$

Each term in the right side of Equation (13) is the function of each independent variable and Equation (13) means that the sum of each term becomes constant. Hence, each term in the right side must be constant.

$$\frac{1}{X(x)}\frac{d^2X(x)}{dx^2} = -k^2, \frac{1}{Y(y)}\frac{d^2Y(y)}{dy^2} = -l^2, \frac{1}{Z(z)}\frac{d^2Z(z)}{dz^2} = -m^2 \tag{14}$$

And Equation (13) becomes as follows.

$$\mu\frac{\alpha+\beta-\mu}{\beta-\mu} = k^2 + l^2 + m^2 \tag{15}$$

From Equation (15), once k, l and m are given, μ can be determined and μ has two values. k, l and m can be determined using the initial and boundary conditions. The details of the further calculations will be shown in the Appendix. The analytic solution is as follows.

$$u = \sum_{i,j,n=1}^{\infty}\left(A_{ijn}^{+}\cdot\exp\left(-\mu_{ijn}^{+}\cdot\tau\right) + A_{ijn}^{-}\cdot\exp\left(-\mu_{ijn}^{-}\cdot\tau\right)\right) \times\cdot\cos\left(\frac{2i-1}{2b}\pi x\right)\sin\left(n\pi y\right)\cdot\cos\left(\frac{2j-1}{2h}\pi z\right) \tag{16}$$

$$v = \sum_{i,j,n=1}^{\infty}\left(\frac{\alpha}{\beta-\mu_{ijn}^{+}}A_{ijn}^{+}\cdot\exp\left(-\mu_{ijn}^{+}\cdot\tau\right) + \frac{\alpha}{\beta-\mu_{ijn}^{-}}A_{ijn}^{-}\cdot\exp\left(-\mu_{ijn}^{-}\cdot\tau\right)\right) \times\cos\left(\frac{2i-1}{2b}\pi x\right)\cdot\sin\left(n\pi y\right)\cdot\cos\left(\frac{2j-1}{2h}\pi z\right) \tag{17}$$

Here, μ_{ijn}^{+} and μ_{ijn}^{-} are the real roots of the following Equation (18) and both roots are always positive because of $\alpha > 0$ and $\beta > 0$.

$$\mu^2 - (\alpha+\beta+k^2+l^2+m^2)\mu + \beta(k^2+l^2+m^2) = 0 \tag{18}$$

The coefficients, A_{ijn}^{+} and A_{ijn}^{-}, are defined by the following system of equations.

$$A_{i,j,n}^{+} + A_{i,j,n}^{-} = \frac{32}{(2i-1)(2j-1)n\pi^3}\sin\left(\frac{2i-1}{2b}\pi w\right)\left(1-\cos\left(n\pi d\right)\right)\left(-1\right)^{j+1} \tag{19}$$

$$\frac{\alpha}{\beta-\mu_{i,j,n}^{+}}A_{i,j,n}^{+} + \frac{\alpha}{\beta-\mu_{i,j,n}^{-}}A_{i,j,n}^{-} = \frac{32v_0}{(2i-1)(2j-1)n\pi^3}\times\sin\left(\frac{2i-1}{2b}\pi w\right)\left(1-\cos\left(n\pi d\right)\right)\left(-1\right)^{j+1} \tag{20}$$

From Equation (20), it is seen that A_{ijn}^{+} and A_{ijn}^{-} depend on the initial content of trapped hydrogen atoms, v_0. By changing v_0, we can examine the effect of the initial distribution on the hydrogen evolution curves.

In this work, we measured the evolution curves, but we did not measure the hydrogen distribution in the specimen each time. Hence, to compare the calculations and the experiments, we would like to integrate Equations (16) and (17) to obtain the total hydrogen inside the specimen, u_T, and we obtain the following.

$$u_T = \sum_{i,j,n=1}^{\infty}\left(\frac{\alpha+\beta-\mu_{i,j,n}^{+}}{\beta-\mu_{i,j,n}^{+}}A_{i,j,n}^{+}\exp(-\mu_{i,j,n}^{+}\tau) + \frac{\alpha+\beta-\mu_{i,j,n}^{-}}{\beta-\mu_{i,j,n}^{-}}A_{i,j,n}^{-}\exp(-\mu_{i,j,n}^{-}\tau)\right) \times\frac{16bh}{(2i-1)(2j-1)n\pi^3}\left(-1\right)^{i+j}\left(1+\left(-1\right)^{n+1}\right) \tag{21}$$

Since the amount of initial hydrogen inside the specimen at $t = 0$ is $(1 + v_0)4wdh$, the amount of hydrogen atoms released from the specimen is calculated as the difference between this value and Equation (21).

4.3 Comparisons of calculations with the experimental results

Here, we compare the hydrogen evolution curves calculated with Equation (21) with the experiments. From the specimen size used in this study, we set a, $2b$' and $2h$' at 10 mm, 25 mm and 40 mm, respectively. In addition, from the cross-section appearance shown in Figure 1 we set $2w$' and d' at 9.5 mm and 1.6 mm, respectively. The next physical property we have to determine is D. In the present work, since the hydrogen evolution was very rapid, we could not determine the diffusion coefficient of the martensitic structure (Specimen C). So, we set D at 0.0002 mm^2/s from the previous work [6]. This value was measured using the HAZ simulated specimen. So the microstructures may not be the same. But since no data were available, we decided to use this value.

Equation (21) can consider the effect of v_0. However, as mentioned already, the value of v_0 is not clear in the case of welded joints. So, for the first calculation, we assume that v_0 is considerably lower than the equilibrium state, $v_0 = \alpha / \beta$. This assumption is that very few hydrogen atoms are initially trapped. We assume that $v_0 = 1.0$, and the values of α and β were determined to make the calculations agree with the experiments. Since α is generally higher than β, this assumption means that the initial hydrogen atoms are not in thermal equilibrium.

Figure 6 shows the comparisons of the calculations and the experiments. In Figure 6, $\alpha = 10.0$ and $\beta = 0.04$ for Specimen A, and $\alpha = 3.0$ and $\beta = 0.04$ for Specimen B are selected ($v_0 = 0.004$ α / β for Specimen A and $v_0 = 0.013$ α / β for Specimen B). Both of them are much lower than the equilibrium value. The reason why the same value of β was used for both Specimens A and B is that the physical

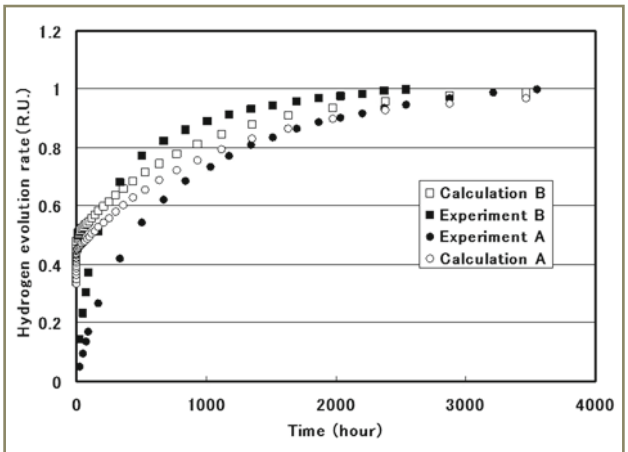

Physical properties used are listed in Table 3. ($\alpha = 10.0$, 3.0 for Calculations A and B, respectively. $\beta = 0.04$ and $\nu_0 = 1$ for both Calculations A and B).

Figure 6 – Comparisons of experiments and calculations

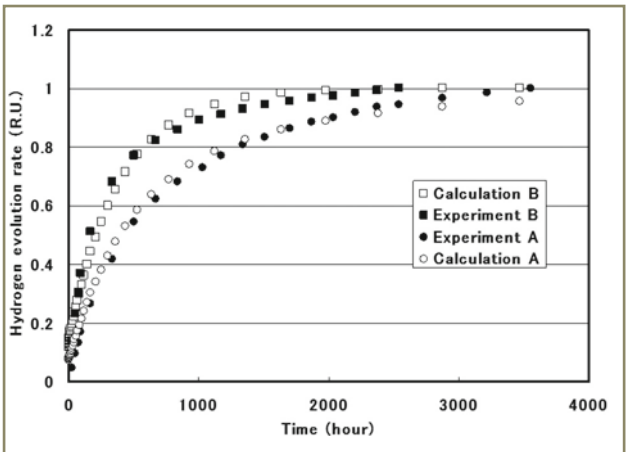

Physical properties used are listed in Table 3. ($\alpha = 50.0$, 5.0 for Calculations A and B, respectively. $\beta = 0.1$ and $\nu_0 = 0.02\ \alpha / \beta$ for both Calculations A and B.)

Figure 7 – Comparisons of experiments and calculations

properties that determine β do not depend on the trap site density, N, while α depends on N. The physical properties used in the calculations are summarized in Table 3.

We tried to make the calculation results fit with the experiments, but the calculations always show the rapid release of hydrogen at the early stage followed by the slow release of hydrogen. In the calculations, the rapid hydrogen release is due to the release of free hydrogen atoms without trapping, and the slow release is due to the trapping and escaping of hydrogen atoms. But the shape of the experimental evolution curves does not agree with that of the calculations. This is probably because the same amount of hydrogen atoms is initially trapped. Hence, in the experiments, it seems that the same amount of hydrogen atoms are trapped at $t = 0$.

Next, we consider the case that the same amount of hydrogen atoms is initially trapped. Here, we assume $\nu_0 = 0.02\ \alpha / \beta$ for both Specimens A and B and determine α and β. Figure 7 shows comparisons of the calculation and experimental results. Contrary to Figure 6, the calculations agree fairly well with the experiments. In Figure 7, we used $\beta = 0.1$ for both Specimens A and B. We used $\alpha = 50.0$ for Specimen A and $\alpha = 5.0$ for Specimen B. From Figures 6 and 7, it is considered that the assumption that very few hydrogen atoms are trapped is not suitable.

4.4 Values of α and β and trap site density, N

In the last section, we have seen that the assumption that the same amount of hydrogen atoms is initially trapped is more suitable to explain the experimental results. Here, we would like to examine the effect of α by comparing the experimental and calculated evolution curves.

The reason why we changed the α value only is that it depends on the trapping densities of Specimens A and B, as seen in Equation (8). In the present work, the retained austenite percentages for Specimens A and B are 16 % and 8 %, respectively. The ratio of the retained austenite percentages is then 2:1. This means that the ratio of α s for Specimens A and B should be also 2:1 if the values of D, k and a are common for Specimens A and B [see the definition of α, Equation (8)]. On the other hand, β does not depend on the trapping density, as seen in Equation (8). Hence, here, we fix $\beta = 0.1$, and change the value of ν_0 to examine the ratio of α s.

Figure 8 shows the calculation results for $\nu_0 = \alpha / \beta$, i.e., the thermal equilibrium condition for the initial state. Here, we treat α as the fitting parameter. The calculation results agree fairly well with the experiments like in Figure 7. But, α s for Specimens A and B are 50.0 and 3.0, respectively, and their ratio is about 17:1. Figure 9 shows the calculation results for $\nu_0 = 0.05\ \alpha / \beta$. Figure 9 also shows

Table 3 – Physical properties used in the calculations

Figure	Specimen	α	β	ν_0	D [mm²/s]
Figure 6	A	10.0	0.04	1	0.0002
	B	3.0			
Figure 7	A	50.0	0.1	0.2 α / β	
	B	5.0			
Figure 8	A	50.0	0.1	α / β	
	B	3.0			
Figure 9	A	50.0	0.1	0.5 α / β	
	B	10.0			

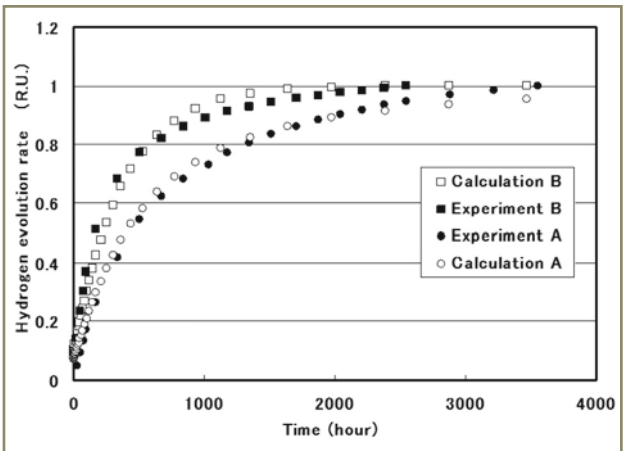

Physical properties used are listed in Table 3. ($\alpha = 50.0$, 3.0 for Calculations A and B, respectively. $\beta = 0.1$ and $\nu_0 = \alpha / \beta$ for both Calculations A and B.)

Figure 8 – Comparisons of experiments and calculations

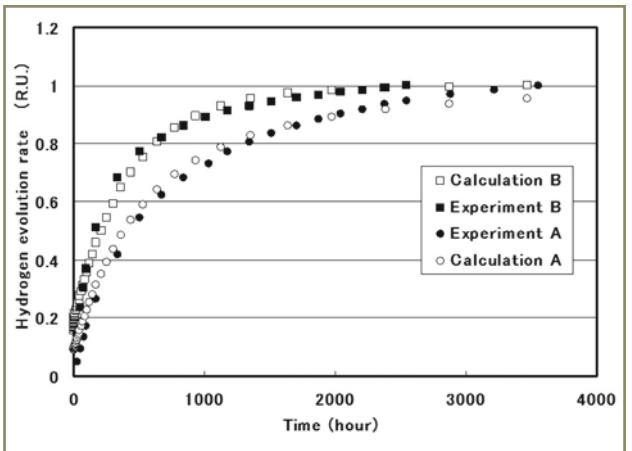

Physical properties used are listed in Table 3. ($\alpha = 50.0$, 10.0 for Calculations A and B, respectively. $\beta = 0.1$ and $\nu_0 = 0.05\ \alpha / \beta$ for both Calculations A and B.)

Figure 9 – Comparisons of experiments and calculations

the fairly good agreement between the experimental and calculation results. α s for Specimens A and B are 50.0 and 10.0, respectively, and their ratio is 5:1. The ratio of α s for Specimens A and B in Figure 7 is 10:1, and the ratio in Figure 6 is about 3:1. Table 4 summarizes the values of α and the ratios. From Table 4, as the initial condition approaches the thermal equilibrium state, the ratio of α s tends to diverge from the experimental result, 2:1. But, as seen in Figure 6, the low value of ν_0 tends to produce a shape of the evolution curves that differs from the experimental results.

From Figure 7 to 9, it seems to be possible to make the calculation results agree with the experiments by modifying the α and β values regardless of the initial hydrogen distribution. But the comparisons of the retained austenite ratio show that the α and β values in Figure 6 are more suitable than those in Figures 7 and 8. In this study, the microstructure data (the retained austenite percentages of Specimens A and B are 16 % and 8 %, respectively) were used to show this point. This also means that the reliability of the α and β values determined only from the hydrogen diffusion data is not good, and that the conventional Fick's Equation is not suitable because of its local equilibrium assumption.

These considerations assume that the trap site density of Specimen A is different from that of Specimen B and that the other physical properties such as the depth of the trap sites are the same. The value of β depends on the depth of the trap site. And in case that β of both Specimens is not the same, the above consideration is not clear. However, the further discussion by the present experimental results is difficult. So additional experiments such as experimental observation of α & β and the diffusion analysis with them are desired.

5 Conclusions

In this work, we measured the hydrogen evolution curves of the weld metals that contain the retained austenite, and compared them with the calculation results using McNabb & Foster Equation. The conclusions obtained are listed below.

1. The hydrogen release time from Specimens A and B that contain retained austenite was more than 100 days. The hydrogen release time of Specimen C was about two days, which agrees with 72 h holding times required by JIS Z3118.
2. We derived the analytic solution of McNabb & Foster Equation for the present experiments. The assumption that the initial trapped hydrogen content is much less than the thermal equilibrium value yields the rapid hydrogen release at the early stage and the slow release at the late stage. The calculated evolution curves, in this case, do not agree with the experiments.
3. The assumption that the same amount of hydrogen is trapped at $t = 0$ produces evolution curves that agree with the experiments. But, the ratio of retained austenite percentages of Specimens A and B determined from the calculation results tends to diverge from the

Table 4 – Ratio of the retained austenite percentages calculated from the values of α

Physical properties	Figure number				X-ray measurement
	8	7	9	6	
ν_0	α / β	0.2 α / β	0.5 α / β	1	-
α for Specimen A	50.0	50.0	50.0	10.0	-
α for Specimen B	3.0	5.0	10.0	3.0	-
Ratio	17:1	10:1	5:1	3:1	2:1

experimental results as the initial trapped hydrogen content becomes high.

Acknowledgements

This study was carried out as a part of research activities of "Fundamental Studies on Technologies for Steel Materials with Enhanced Strength and Functions" by Consortium of JRCM. Financial support from NEDO is gratefully acknowledged. The authors also greatly appreciate the help of Prof. Saida at Osaka University for the measurements of the retained austenite percentages.

References

[1] Bailey N., Coe F., Gooch T., Hart P., Jenkins N. and Pargeter R.: Welding steels without hydrogen cracking, Abington Publishing and ASM International, 1973, p. 67.

[2] Yara H., Makishi Y., Kikuta Y. and Matsuda H.: Mechanical and metallurgical properties of trial covered electrode, Quaterly Journal of the Japan Welding Society, 1987, vol. 5, no. 1, pp. 108-112.

[3] McNabb A. and Foster P.R.: A new analysis of the diffusion of hydrogen in iron and ferritic steels, Transactions of the Metallurgical Society of AIME, 1963, vol. 227, no. 3, pp. 618-27.

[4] Crank J.: The mathematics of diffusion, Claredon Press, Oxford, 1975.

[5] Carslaw H.S. and Jaege J.C.: Conduction of heat in solids, 2nd ed., Oxford University Press, Oxford, 1959.

[6] Okumura M., Kasuya T., Yurioka N. and Nagano K.; Effect of cleanliness of steel on its weldability, Quaterly Journal of the Japan Welding Society, 1988, vol. 6, no. 1, pp. 144-150.

Appendix

Here, we would like to derive Equations (16), (17) and (18). At first, from Equation (14), we obtain

$$X(x) = A\cos(kx),\ Y(y) = B\sin(ly),\ Z(z) = C\cos(mz) \quad (22)$$

Here, we selected the cosine function for $X(x)$ and $Z(z)$ by considering the symmetry of the model, and the sine function for $Y(y)$ by considering the boundary condition at $y = 0$. Since the hydrogen content is zero at $x = b$ and $z = h$, we obtain

$$\cos(kb) = 0, \text{ hence, } k = \frac{2i-1}{2b}\pi,\ (i = 1,2,3,,,) \quad (23)$$

$$\cos(mh) = 0, \text{ hence, } m = \frac{2j-1}{2h}\pi,\ (j = 1,2,3,,,) \quad (24)$$

In addition, the hydrogen content is also zero at $y = 1$,

$$\sin(l) = 0, \text{ hence, } l = n\pi,\ (n = 1,2,3,,,) \quad (25)$$

By rewriting the coefficients in Equation (24), we obtain,

$$u = \exp(-\mu\tau)A_{ijn}\cos\left(\frac{2i-1}{2b}\pi x\right)\sin(n\pi y)\cos\left(\frac{2j-1}{2h}\pi z\right) \quad (26)$$

$$v = \frac{\alpha}{\beta-\mu}u \quad (27)$$

The value of μ is given by Equation (18), and this quadratic equation gives the two real roots. When we put $\omega^2 = k^2 + l^2 + m^2\ (>0)$, since $\alpha > 0$ and $\beta > 0$, the discriminant of this equation is;

$$(\alpha+\beta+\omega^2)^2 - 4\beta\omega^2 = \{\omega^2 + (\alpha-\beta)\}^2 + 4\alpha\beta > 0 \quad (28)$$

Hence the two roots of Equation (18) are real. Furthermore, these two roots are positive. To explain this, we regard the left side of Equation (18) as the quadratic function of μ. In this case, the vertical line of this function is $\mu = (\alpha+\beta+\omega^2)/^2\ (>0)$ and the value of this function at $\mu = 0$ is $\beta\omega^2\ (>0)$. These mean that the two roots are positive. So, we describe these two positive roots as $\mu_{ijn}{}^{+}$ and $\mu_{ijn}{}^{-}$. Equations (26) and (27) satisfy the McNabb & Foster Equation for each $\mu_{ijn}{}^{+}$ or $\mu_{ijn}{}^{-}$, and since both Equations (26) and (27) are linear, the linear combinations of the equations also satisfy the McNabb & Foster Equation. Hence, u and v can be described as Equations (16) and (17), respectively. In Equations (16) and (17), since one set of (i, j, n) produces two different μ, we add the suffix notation, $\pm$. $A_{ijn}{}^{+}$ and $A_{ijn}{}^{-}$ can be determined by the initial condition by using the orthogonality of the trigonometric function. Substituting Equation (16) into Equation (9) and setting $\tau = 0$, we conducted the integration by multiplying both sides by $\cos\left(\frac{2i'-1}{2b}\pi x\right)\sin(n'\pi y)\cos\left(\frac{2j'-1}{2h}\pi z\right)$. Then, the integrations except the cases of $i = i'$, $j = j'$ and $n = n'$ become zero and Equation (19) is obtained. In this calculation, we used the following equations.

$$\int_0^b \cos^2\left(\frac{2i-1}{2b}\pi x\right)dx = \frac{b}{2},\ \int_0^b \cos^2\left(\frac{2j-1}{2h}\pi z\right)dz = \frac{h}{2},$$

$$\int_0^1 \sin^2(n\pi y)\,dy = \frac{1}{2}$$

$$\int_{-w}^{w}\cos\left(\frac{2i-1}{2b}\pi x\right)dx\int_0^d \sin(n\pi y)\,dy\int_{-h}^{h}\cos\left(\frac{2j-1}{2h}\pi z\right)dz$$
$$= \frac{16bh}{(2i-1)(2j-1)n}\frac{1}{\pi^3}(-1)^{j+1}\sin\left(\frac{2i-1}{2b}\pi w\right)\left(1-\cos(n\pi d)\right)$$

By the similar calculation, we obtained Equation (20).

The hydrogen evolution curve can be calculated using Equations (19) and (20). We have to calculate the total amount of hydrogen inside the specimen, u_T, and this is calculated as

$u_T = \int_{-b}^{b} dx \int_{0}^{1} dy \int_{-h}^{h} dz(u+v)$ that yields Equation (21). To conduct this integration, we used the following equation.

$$\int_{-b}^{b} \cos\left(\frac{2i-1}{2b}\pi x\right) dx = \frac{4b}{(2i-1)\pi}(-1)^{i+1}, \int_{0}^{1} \sin(n\pi y)\, dy = \frac{1}{n\pi}\left(1+(-1)^{n+1}\right)$$

Equation (21) gives the total amount of hydrogen existing inside the specimen. The total amount of hydrogen escaping from the specimen can be calculated as Equation (29). Here, we used the initial amount of hydrogen inside the specimen is $(1 + v_0)(2h)\,(2w)d$.

$$F = 1 - \frac{u_T}{(1+v_0)(2w)(2h)d} \tag{29}$$

About the authors

Dr. Tadashi KASUYA (kasuya@mat.eng.osaka-u.ac.jp), formerly with Welding and Joining Research Center, Nippon Steel Corporation, Chiba (Japan) is now with Osaka University, graduate school of Engineering, Osaka (Japan). Mr. Yuji HASHIBA (hashiba.yuji@nsc.co.jp, and Dr. Hiroshige INOUE (inoue.hiroshige@nsc.co.jp) are both with Welding and Joining Research Center, Nippon Steel Corporation, Chiba (Japan).